

Influence of α -cluster in light nuclei on di-hadron azimuthal correlation in relativistic heavy-ion collisions

Yuan-Zhe Wang (王远哲), Song Zhang (张松),* and Yu-Gang Ma (马余刚)[†]
*Key Laboratory of Nuclear Physics and Ion-beam Application (MOE),
 Institute of Modern Physics, Fudan University, Shanghai 200433, China*

We investigate the effect of α cluster in relativistic collisions via di-hadron azimuthal correlation. A collision system scan involving α -clustered ^{12}C and ^{16}O is studied by using a multiphase transport model in the most central collisions at $\sqrt{s_{NN}} = 6.37$ TeV. We compare the correlation functions of different configurations and calculate root-mean-square width and kurtosis in the away-side region. The momentum dependence of di-hadron azimuthal correlation is also presented. The results show substantial distinction in correlation functions between Woods-Saxon distribution and α -clustered structures. We argue that the difference related to jet quenching is originated from initial geometry anisotropy. This work proposed that di-hadron azimuthal correlation is a potential probe to distinguish α -clustered nuclei.

I. INTRODUCTION

α cluster model has attracted much attention [1] since it was postulated by Gamow [2]. Both theoretical and experimental efforts provided crucial evidence for the formation of α -particle condensates in light self-conjugate nuclei [3–5], one of the most famous work was the Hoyle state of ^{12}C [6]. Possible α cluster model of heavy nuclei has also been studied [7]. Compared with classical Woods-Saxon distribution, α -clustering structure nuclei emerge a deformed intrinsic configuration. The ground state of α -clustered ^{12}C is suggested to show a triangular-like arrangement, while α -clustered ^{16}O has a tetrahedron structure [8–12]. Specific spatial nucleon distribution incite us to search for different physical features between clustered nuclei and non-clustered cases. For example, our previous works demonstrated the effects of α -clustering structure on giant dipole resonance [9] and photonuclear reactions [13, 14].

It was proposed that we could distinguish initial nuclear structure via high energy heavy-ion collisions [15]. This methodology originates from hydrodynamic calculations, which demonstrate that the asymmetry of the initial coordinate space shall turn into the momentum space anisotropy in the evolution of deformed fireball whose shape relates to original nucleon distribution [16–19]. Many work focus on collective flow suggested in Ref. [15], revealing evidential distinction between uniform and clustered nuclei [11, 20–22].

Moreover, we can deduce the information in the early stage by studying jet quenching phenomenon as well [23–26]. In ultra-relativistic heavy-ion collisions, participants melt into deconfined quarks and gluons, leading to production of the hot dense matter so-called quark-gluon plasma (QGP). Energetic partons created in hard scattering are believed to lose considerable energy when they

traverse the dense medium. The energy loss is sensitive to path length [23] and results in many consequential observables, for instance, the strong suppression on the yields of away-side high p_T particles [27, 28]. Even though the detailed mechanism of jet quenching is still under debate, such a phenomenon gives clues on the collective motion of QGP and is expected to reflect properties of the pre-collision system. However, it is difficult to detect the jet fragmentation process directly, whereas di-hadron azimuthal correlation distribution is a widely used method to reconstruct the picture of jet signals [29–31].

Over the past decades, there have been numerous experiments that carried out di-hadron azimuthal correlation measurements at various center-mass energies and collision systems [24, 32–38]. It was found that small collision systems such as p + p and p + A in high-multiplicity present resembling properties with large A + A collisions [39]. Due to minor size and short lifetime, small-size A+A systems may undergo a modified dynamical process and are expected to shed light on initial fluctuation effects on momentum distribution in the final stage [25, 26, 40–42].

To investigate the influence on di-hadron azimuthal correlations from the intrinsic geometry in α -clustered nuclei, a multi-phase transport (AMPT) model [43] was employed to simulate a system scan of symmetric collision systems from $^{10}\text{B} + ^{10}\text{B}$ to $^{197}\text{Au} + ^{197}\text{Au}$ in most central collisions (impact parameter $b = 0$ fm) at $\sqrt{s_{NN}} = 6.37$ TeV. The di-hadron azimuthal correlation functions were calculated and the background with respective to different order event-/participant- plane were reconstructed. Based on the correlation functions, the system size dependence of the root-mean-square width and kurtosis in the away-side region is discussed. These results shed light on the future system scan project at RHIC and LHC [44, 45], and also proposed as a probe to distinguish the α -clustering structure in light nuclei, such as ^{12}C and ^{16}O .

The paper is arranged as follows: In Sec. II, we introduce the AMPT model and the procedures for evaluating

* song_zhang@fudan.edu.cn

[†] mayugang@fudan.edu.cn

di-hadron azimuthal correlation. The correlation results and discussions are placed in Sec. III. Several relevant cumulants focusing on the away-side associated particle yields are presented simultaneously. Finally we give a summary in Sec. IV.

II. AMPT MODEL AND ANALYSIS METHODS

In this work, we use a multiphase transport model (AMPT) [43, 46] to perform calculation in most central collision systems. The AMPT model consists of four main components, which describe the four main processes in heavy ion collisions. The initial conditions including the generation of partons are simulated by the Heavy Ion Jet Interaction Generator (HIJING) model [47, 48], the partonic interactions is modelled with Zhang's parton cascade (ZPC) model [49], the hadronization process is carried through a quark coalescence model, and finally the hadron scattering is described by A Relativistic Transport (ART) model [50]. There are two versions of AMPT: one for a string melting mechanism, in which a partonic phase is generated from excited strings in the HIJING model, and a simple quark coalescence model is used to combine the partons into hadrons; the other for the default AMPT version which only undergoes a pure hadron gas phase. AMPT model has been widely used in heavy ion collision at RHIC and LHC [43, 46, 51–54] and the detailed introduction can be found therein. In the present work, we use the string-melting version AMPT.

The nucleon distribution of ^{12}C and ^{16}O are set up in initial state of the AMPT model. While the Woods-Saxon distribution particles are introduced from the HIJING model, the original parameters of α -clustered nuclei are calculated by the EQMD model [55] with effective Pauli potential. In order to match the experimental data [56], vertexes where α cluster lays in the triangular-like ^{12}C are placed 3.10 fm away from each other [9, 21]. For the tetrahedral pattern of ^{16}O , we assign the side length as 3.42 fm [57, 58]. Meanwhile, α clusters are formed by nucleons with Woods-Saxon distributions. For each clustered nucleus we set a random orientation.

At the early stage of the relativistic heavy-ion collisions, jets are always produced back-to-back on the transverse plane in the hard scattering processes [59]. The particle in the jets will loss part of its energy through the interactions while passing through the matter created in the collisions, which is called the well-known jet quenching [23, 60–62]. The energy and momentum will be redistributed via the interaction between the jets and the medium and then the correlation emerges among the particles. Di-hadron azimuthal correlation proved to describe the correlations is constructed by paired hadrons, where a high p_T hadron denoted as a trigger particle stemming from hard scattering processes and a lower p_T hadron as an associated particle which may inherit energy or momentum from the trigger particle. The di-hadron azimuthal correlation is defined as

$\Delta\phi = \phi_{\text{asso}} - \phi_{\text{trig}}$ distribution,

$$C(\Delta\phi) = \frac{1}{N_{\text{trig}}} \frac{dN}{d\Delta\phi}, \quad (1)$$

where N_{trig} is the number of trigger particles, ϕ_{asso} and ϕ_{trig} are the azimuthal angle of the associated particle and the trigger particle, respectively.

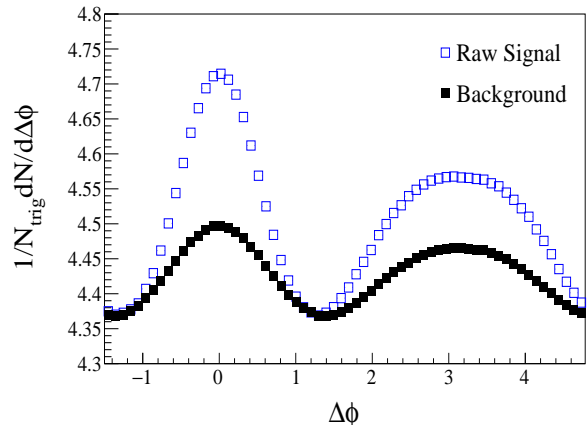


FIG. 1. Di-hadron azimuthal correlation signal (open circles) and background (solid squares) reconstructed by mix-events method in $^{16}\text{O} + ^{16}\text{O}$ collisions at $\sqrt{s_{NN}} = 6.37$ TeV with $b = 0$ fm, both are divided by total numbers of trigger particles in all events. The background of per-trigger yields $\Delta\phi$ distribution is reconstructed by mixing events with similar event plane and normalized with ZYAM method.

The most significant background in the correlations comes from the collective flow, which can be expanded as [63],

$$f(\Delta\phi) \propto \left[1 + \sum_{n=1}^{\infty} 2\langle v_n^a v_n^b \rangle \cos(n\Delta\phi) \right], \quad (2)$$

where v_n^a and v_n^b are n -th order collective flow coefficients of trigger and associated particles. To estimate this background $\Delta\phi$ distribution, a mixed-event method was used [64, 65] as following: the trigger particle and associated particle are from different events which have similar event properties, such as the second and third order event plane angles which will be introduced later. Note that all collision systems we used in this analysis are the most central collisions with a impact parameter $b = 0$ fm. The effect of multiplicity or the centrality, therefore, is negligible in the mixed-event method. In practice, $dN_{\text{mixed}}/d\Delta\phi$ and $dN_{\text{same}}/d\Delta\phi$, denote the $\Delta\phi$ distributions from mixed events and same events, respectively, and then the real signal of correlation function (1) is obtained via $C(\Delta\phi) = 1/N_{\text{trig}}(dN_{\text{same}}/d\Delta\phi - B_0 * dN_{\text{mixed}}/d\Delta\phi)$, where B_0 is a normalizing factor by a so-called ZYAM method [30] (zero yield at minimum). To illustrate the ZYAM method, figure 1 shows the correlation function constructed in the same event (raw signal) and mixed events (background), respectively, in ^{16}O

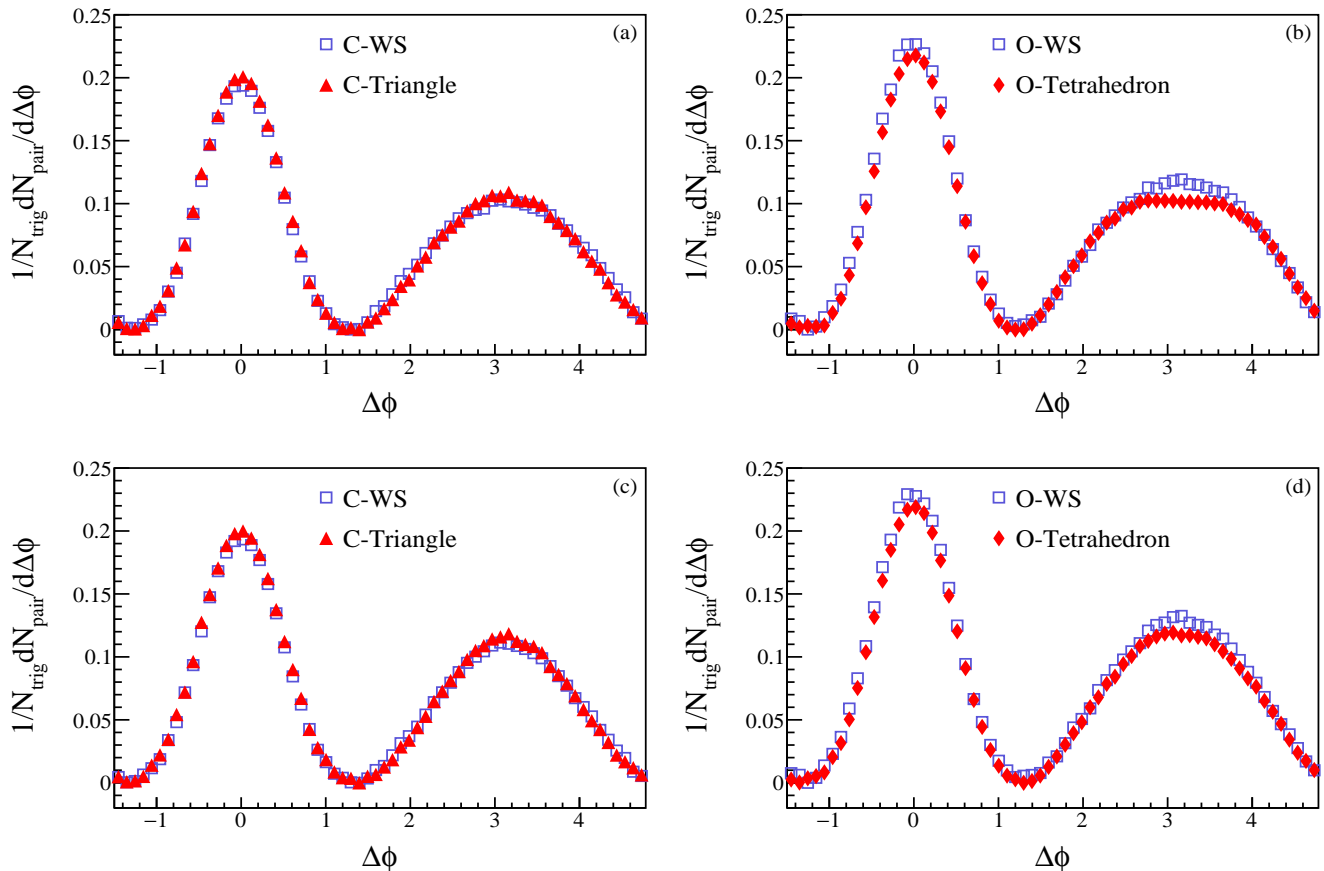


FIG. 2. Subtracted di-hadron azimuthal correlation function in $^{12}\text{C} + ^{12}\text{C}$ (left panel) and $^{16}\text{O} + ^{16}\text{O}$ (right panel) collision systems at $\sqrt{s_{NN}} = 6.37$ TeV with $b = 0$ fm. Open squares represent the Woods-Saxon distribution for nucleus in both systems, red triangles for triangular 3α -clustered ^{12}C , and red diamonds for the ^{16}O with tetrahedron 4α arrangement. Panel (a) and (b) use event plane method, (c) and (d) use participant plane method.

+ ^{16}O collisions at $\sqrt{s_{NN}} = 6.37$ TeV. The normalizing factor B_0 can be tuned to get zero yield in the correlation function $C(\Delta\phi)$ in a region of $0.8 < \Delta\phi < 1.2$.

An approach to estimate the reaction plane is the event plane method gained by the orientation of the flow vector [66]. The n -th order event plane angle is defined as,

$$\Psi_n^{\text{EP}} = \tan^{-1} \left(\frac{\sum_i \sin(n\phi_i)}{\sum_i \cos(n\phi_i)} \right), \quad (3)$$

where ϕ_i is the azimuthal angle of particle i , the sum runs over all emitted particles in the event. Instead of event plane, the participant plane method that utilizes the information of participant zone is also effective [67]. The participant plane angle is given as,

$$\Psi_n^{\text{PP}} = \frac{\tan^{-1} \left(\frac{\langle r_{part}^2 \sin(n\phi_{part}) \rangle}{\langle r_{part}^2 \cos(n\phi_{part}) \rangle} \right) + \pi}{n}, \quad (4)$$

where r_{part} and ϕ_{part} are polar coordinate positions of the initial partons instead of participants to consider the

initial fluctuations in the transverse plane, the average $\langle \dots \rangle$ takes over all initial partons. We adopt both methods in this work to confirm the results.

III. RESULTS AND DISCUSSION

The di-hadron azimuthal correlations are calculated in the most central ($b=0$ fm) A + A collisions with kinetic windows, rapidity in $|y| < 1$, transverse momentum $2 < p_T < 6$ GeV/ c for the trigger particle and $0.2 < p_T < 2$ GeV/ c for associated particles. And the charged hadrons π^\pm , K^\pm , p and \bar{p} are selected for this study.

Figure 2 shows the background-subtracted correlation functions in central $^{12}\text{C} + ^{12}\text{C}$ collisions on panel (a) and (c), and $^{16}\text{O} + ^{16}\text{O}$ collisions on panel (b) and (d) at $\sqrt{s_{NN}} = 6.37$ TeV, where the collided nuclei are configured in the Woods-Saxon distribution and the α -clustered structure, triangle for ^{12}C and tetrahedron for ^{16}O , respectively. We adopted event plane methods in panel (a) and (b), and participant plane method in panel

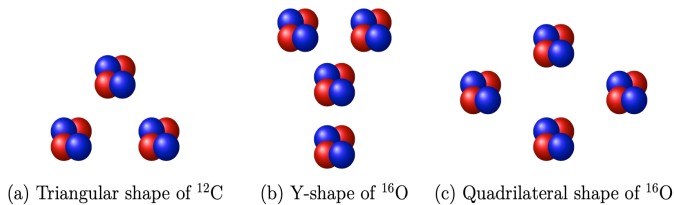


FIG. 3. Schematic illustration of different shapes of clustered nuclei in the transverse plane.

(c) and (d). Noting that the event-/participant- plane angle constructed above are only used in the mixing event procedure for estimating the background. From the di-hadron azimuthal correlation results, the away-side double peak structure which appears in $^{197}\text{Au} + ^{197}\text{Au}$ collisions [33] is absent in the both systems, implying a small system feature of $^{12}\text{C} + ^{12}\text{C}$ and $^{16}\text{O} + ^{16}\text{O}$ collisions. The correlation functions in $^{12}\text{C} + ^{12}\text{C}$ collisions exhibit unobviously difference between the α -clustered triangle structure and the Woods-Saxon distribution as shown in panel (a) and (c). On the away-side ($\Delta\phi \sim \pi$) correlation, the correlation function is suppressed and broadened due to the violent interaction among the back jets and associated particles. The correlation functions in $^{16}\text{O} + ^{16}\text{O}$ collisions present noteworthy differences in different configurations of ^{16}O in panel (b) and (c). In $^{16}\text{O} + ^{16}\text{O}$, both the near-side ($\Delta\phi \sim 0$) and the away-side correlation function are higher in the configuration via the Woods-Saxon distributions than those via the α -clustered tetrahedron structure. By comparing the two collision systems, it is seen that the results depend not only on the size of the collision system but also the initial geometry configurations.

To understand the effect from α -cluster structure on di-hadron azimuthal correlations qualitatively, we can imagine an α -clustered nucleus collides against another in the transverse plane via a geometric figure. The energy density is larger around the vertexes that represent α particles, leading to incident hard scattering process and violent energy loss nearby. We can therefore view α clusters as birthplace and barrier of jets. Moreover, as mentioned in Refs. [15, 20], the orientation of clustered nuclei plays an important role in multiplicity. When the coplane of most vertexes are parallel to transverse plane, the clustered nuclei exhibit the largest overlapped region and produce the most wounded nucleons. And incoming nuclei should keep same orientation with the other to make α particles collide center-to-center directly. This situation, which can obtain the highest multiplicity due to strong damage, should be regarded as the main source of jetlike correlations and studied primarily.

For clustered $^{12}\text{C} + ^{12}\text{C}$ collision systems, the 3α -particle condensates in nucleus construct a triangular figure (Fig. 3(a)) in the transverse plane. When a hard scattering process occurs at a vertex, particles travelling outside straightly are more likely to hold high- p_T

property to be detected. The backside particles which pass through the other two vertexes loss energy furiously. The decrease of associated particles may be related to the sharper away-side peak. For clustered $^{16}\text{O} + ^{16}\text{O}$ collision systems, the two-dimensional projection of 4α -particle condensates has a Y-like or quadrilateral shape in the transverse plane, as shown in Fig. 3(b) and (c). If a trigger particle emerges inside the central vertex of the Y-shape structure, the amount of associated particles in all direction are expected to reduce due to the surrounding dense medium. The decreased yields can result in the suppression of correlation function on the near-side. Furthermore, for jets which travel outwards from other vertexes in both shapes, particles moving along the reverse direction will strike against the backside barriers. As a result, the correlation peak around $\Delta\phi = \pi$ is flatter in the clustered condition.

As discussed above, we observe the discrepancy on away-side di-hadron azimuthal correlation between clustered and uniform nuclei collisions. One question that needs to be asked, however, is whether α clustering structure can be distinguished via di-hadron azimuthal correlations in both $^{12}\text{C} + ^{12}\text{C}$ and $^{16}\text{O} + ^{16}\text{O}$ collisions. Accordingly, we employed a scan of central symmetric collision systems at $\sqrt{s_{NN}} = 6.37$ TeV. Figure 4 gives the correlation function of collision systems with different size. We can find a multi-peak structure on the away-side correlation in large systems such as $^{197}\text{Au} + ^{197}\text{Au}$ and $^{96}\text{Zr} + ^{96}\text{Zr}$ collisions in panel (a). The multi-peak structure is different from our previous work [62], which was due to the mixed-event method to subtract background from the collective flow. In panel (b) the background is reconstructed by mixing events only with the requirement of similar second event plane, and the double-peak structure reappears in large collision systems as that in [62]. However, the triangular flow contribution can result in the valley around $\Delta\phi = \pi$ of di-hadron azimuthal correlation as Eq. (2) reveals. Since the largest multiplicity comes with high triangularity in clustered nuclei collisions [15], especially for ^{12}C with triangle-like arrangement, the influence of triangularity needs to be considered in this work. We adopt the same method like panel (a) in the following calculations.

In order to pinpoint the discrepancy in the shape of correlation functions on the away-side, the following cumulants extracted from away-side di-hadron azimuthal correlation could characterize the distributions quantitatively. The root-mean-square (rms) width [62], which describes the dispersion of the associated particles with respect to the direction of back jet, is defined as

$$\Delta\phi_{\text{rms}} = \sqrt{\frac{\sum_{\text{away}} (\Delta\phi - \Delta\phi_m)^2 (dN/d\Delta\phi)}{\sum_{\text{away}} (dN/d\Delta\phi)}}, \quad (5)$$

where $\Delta\phi_m$ is set as π , and the away-side region used in summation is from 1.5 to $2\pi - 1.5$. Figure 5 shows the system size dependence of away-side rms width with event plane and participant plane method in panel (a) and (b),

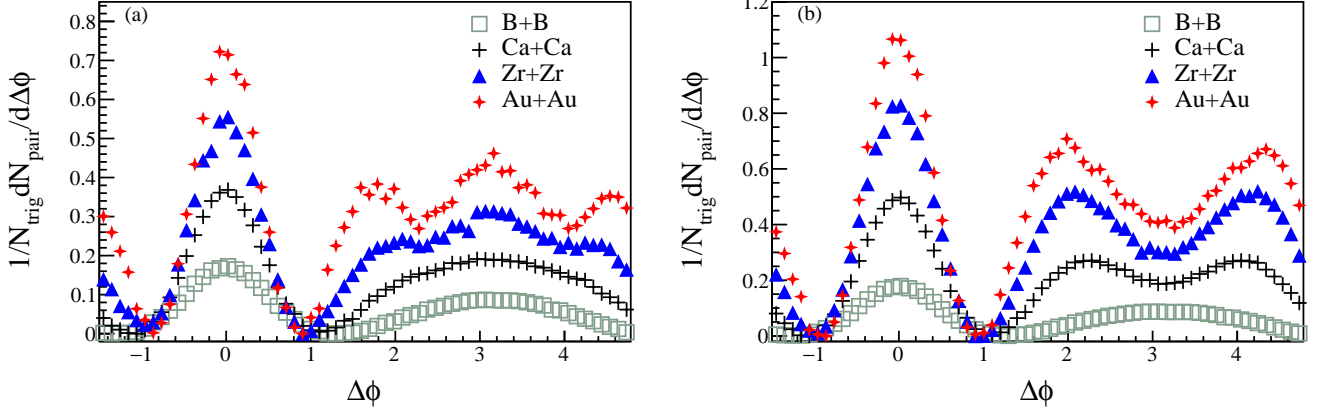


FIG. 4. Subtracted di-hadron azimuthal correlation function in different collision systems of nuclei with Woods-Saxon distributions at $\sqrt{s_{NN}} = 6.37$ TeV with $b = 0$ fm. Green squares for $^{10}\text{B} + ^{10}\text{B}$, black plus for $^{40}\text{Ca} + ^{40}\text{Ca}$, blue triangles for $^{96}\text{Zr} + ^{96}\text{Zr}$, red double-diamond for $^{197}\text{Au} + ^{197}\text{Au}$. Panel (a) requires both the second and the third order event plane, while panel (b) concentrates on the second order.

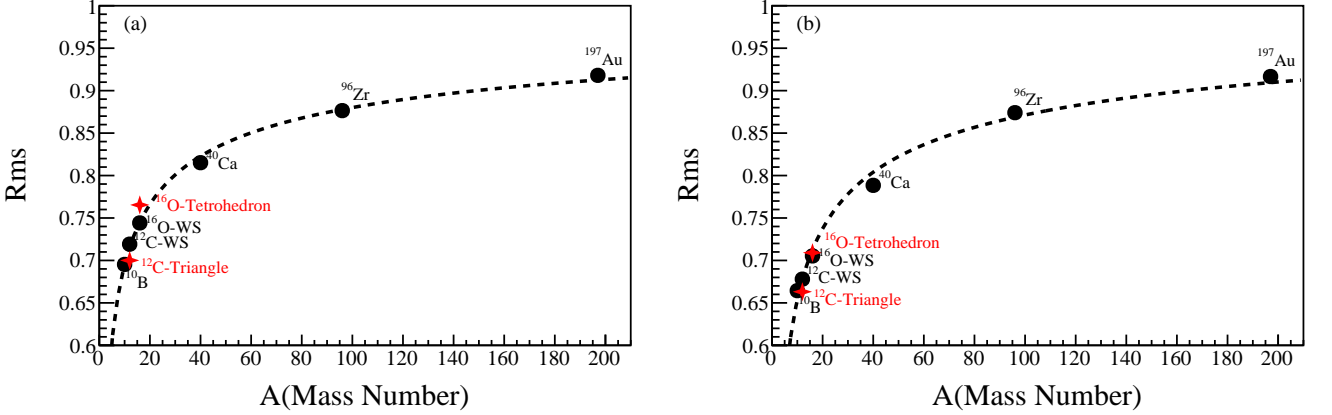


FIG. 5. System scan of away-side RMS width of correlation functions at $\sqrt{s_{NN}} = 6.37$ TeV with $b = 0$ fm. Panel (a) uses event plane method and panel (b) uses participant plane method. The statistical error bars are inside the marker size. The dashed lines are fitted as a function of $k * A^{-1/3} + c$ with $k = -0.745$ and $c = 1.040$ for (a) and $k = -0.877$ and $c = 1.061$ for (b).

respectively. In the collision systems with Woods-Saxon distribution nuclei, the rms width is increasing smoothly with the increase of system size from $^{10}\text{B} + ^{10}\text{B}$ to $^{197}\text{Au} + ^{197}\text{Au}$ collisions, which indicates the broadening distribution of associated particles in larger systems and is consistent with our previous study [62]. It is found that in the two α -clustered nuclei collision systems the rms widths deviate from the dashed line fitted by Woods-Saxon distributions with a function of $k * A^{-1/3} + c$. The α -clustered $^{12}\text{C} + ^{12}\text{C}$ collision has a smaller rms width, while α -clustered $^{16}\text{O} + ^{16}\text{O}$ collision exhibits a larger value. It is found that the differences by event plane method in panel (a) are more significant than that by participant plane method in panel (b), especially in $^{16}\text{O} + ^{16}\text{O}$ collision system, where the rms width difference range between clustered and uniform nuclei is 0.02 in event plane method and 0.004 in participant method.

This indicates the α -cluster structure affects the evolution of the fireball from the system size dependence of the rms width even though the difference between Woods-Saxon case and α -clustered case is not very obvious.

To further investigate the α -clustering effect from the away-side correlation function, another useful observable referred to kurtosis [68], which describes the tailedness of the distribution, is sensitive to correlation yields far from $\Delta\phi_m$ on the away-side. Kurtosis is defined as

$$\Delta\phi_{\text{kurt}} = \frac{\sum_{\text{away}} (\Delta\phi - \Delta\phi_m)^4 (dN/d\Delta\phi)}{\Delta\phi_{\text{rms}}^4 \cdot \sum_{\text{away}} (dN/d\Delta\phi)} - 3, \quad (6)$$

in which the summation takes the same computing steps as rms width. This definition sets the kurtosis of normal distribution equal to zero. The results of kurtosis in different systems are displayed in Fig. 6. All negative

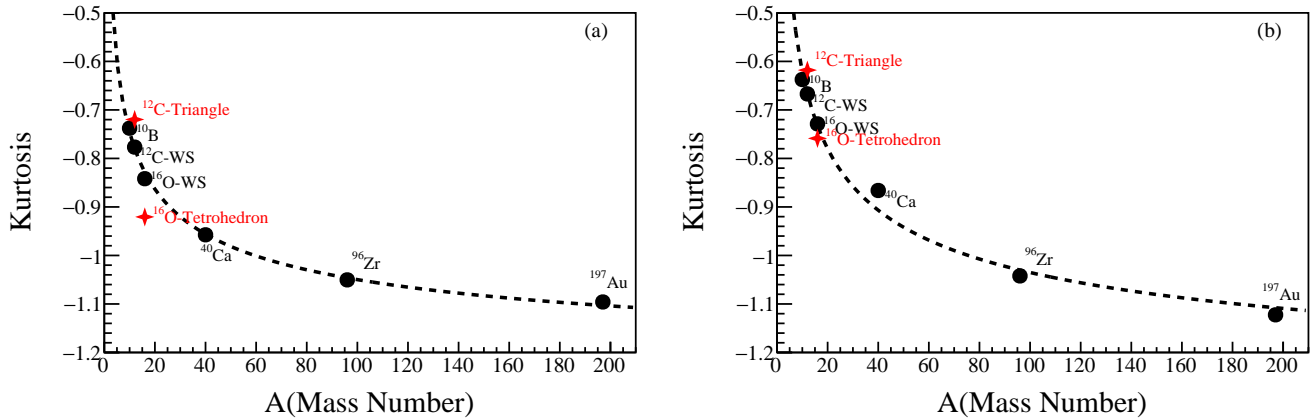


FIG. 6. System scan of away-side Kurtosis of correlation functions at $\sqrt{s_{NN}} = 6.37$ TeV with $b = 0$ fm. Panel (a) uses event plane method and panel (b) uses participant plane method. The statistical error bars are inside the marker size. The dashed lines are fitted as a function of $k * A^{-1/3} + c$ with $k = 1.220$ and $c = -1.313$ for (a) and $k = 1.667$ and $c = -1.394$ for (b).

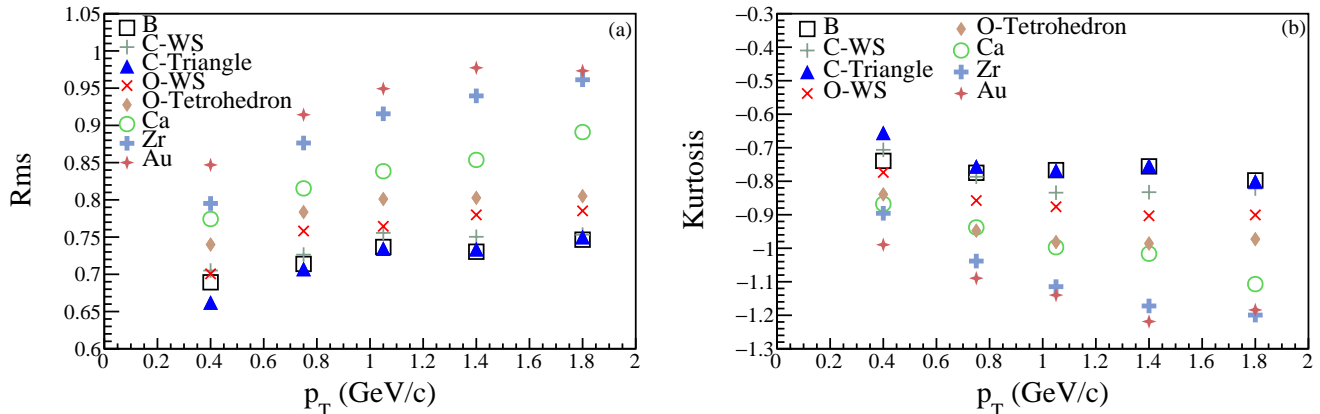


FIG. 7. Rms width (a) and kurtosis (b) versus p_T^{asso} from $^{10}\text{B} + ^{10}\text{B}$ to $^{197}\text{Au} + ^{197}\text{Au}$ collision systems at $\sqrt{s_{NN}} = 6.37$ TeV with $b = 0$ fm. Both panels use event plane method.

values of kurtosis for different collision systems illustrate that the away-side di-hadron distribution widths are all wider than the Gaussian distribution. And a clear trend of decreasing kurtosis with increasing system size in uniform heavy ion collision systems demonstrates that the flattening correlation peak on the away-side, especially the augmenting associated particles perpendicular to the direction of jet. It is noticeable that the disparity of kurtosis between clustered and uniform nuclei is more remarkable than rms width. It means that the kurtosis of away-side di-hadron correlation could be more capable of separating out clustered nuclei. A comparison of panel (a) and (b) reveals the obvious changes of kurtosis in smaller collision systems until $^{40}\text{Ca} + ^{40}\text{Ca}$, while larger systems like $^{96}\text{Zr} + ^{96}\text{Zr}$ and $^{197}\text{Au} + ^{197}\text{Au}$ keep almost the same value. The differences may be generated from incomplete transformation from the initial fluctuation to collective flow in small systems [69, 70].

The α -clustering effects on di-hadron azimuthal correlation preserve a wide range of the transverse momentum. Here, we select the trigger particle with $2 < p_T < 6$ GeV/c, and change the momentum range of associated particles continuously. The background of di-hadron correlation is evaluated with event plane method. In Fig. 7(a) the Rms widths increase with the increasing of transverse momentum of associated particles in all collision systems. From Fig. 7(b), the kurtosis is expected to decline gradually with the increasing of transverse momentum of associated particles and tends to reach a constant in small collision systems. Although the paired particles are selected with different momentum, the magnitude relation among common collision systems does not change in general. The larger collision system has larger rms width and lower kurtosis. Clustered and uniform distribution of ^{12}C and ^{16}O also can be identified just by the value of kurtosis as well as rms width. Indeed, we

demonstrate that the range of p_T^{asso} is irrelevant to the differences of different nuclei in the shape of away-side correlation functions.

IV. SUMMARY

This paper set out to determine the effect of α cluster on di-hadron azimuthal correlation, and provided relevant observable for α -cluster for experimental analysis. By using AMPT model, we calculated di-hadron azimuthal correlation and reconstructed the background from collective flow by mixed-event method with second and third event-/participant plane angle taking into account. Via ZYAM method the background was subtracted from the raw signals to obtain the correlation functions. The associated particle distributions on the away-side of the correlation functions in $^{12}\text{C} + ^{12}\text{C}$ and $^{16}\text{O} + ^{16}\text{O}$ collision system are sensitive to the initial geometry, namely the α -clustering structure configurations, which were related to the path length along which the energetic particles pass through the medium created in the collision. The evolution of the dense medium made the spatial anisotropy transform to the momentum space, especially the broadening of away-side correlation structures.

We also investigated the system size and associated

particle momentum dependences of correlation functions by computing root-mean-square width and kurtosis which characterized the shape of away-side correlation, respectively. The manifestation of α -clustered nuclei with varying system showed a significant divergence with respect to uniform nuclei. The independence with momentum on the relation among different systems strengthened the applicability of di-hadron azimuthal correlation to probe the α -clustering structure in relativistic heavy-ion collisions. However, it is still an open question of the mechanism causing to different variation tendency between small systems and large systems. A system scan project is expected to reveal the properties of the evolution of the phase-space from initial to final state in the collisions as well as to distinguish the exotic nuclear structures.

ACKNOWLEDGMENTS

This work was supported in part by the National Natural Science Foundation of China under contract Nos. 11875066, 11890710, 11890714, 11925502, 11961141003, National Key R&D Program of China under Grant No. 2018YFE0104600 and 2016YFE0100900, the Strategic Priority Research Program of CAS under Grant No. XDB34000000, and Guangdong Major Project of Basic and Applied Basic Research No. 2020B0301030008.

-
- [1] M. Freer, H. Horiuchi, Y. Kanada-En'yo, D. Lee, and U.-G. Meißner, *Reviews of Modern Physics* **90**, 035004 (2018).
 - [2] G. Gamow, *Constitution of Atomic Nuclei and Radioactivity* (Clarendon Press, Oxford, 1931).
 - [3] C. Beck, ed., *Clusters in Nuclei*, Lecture Notes in Physics (Springer Berlin Heidelberg, Berlin, Heidelberg, 2010).
 - [4] A. Tohsaki, H. Horiuchi, P. Schuck, and G. Röpke, *Physical Review Letters* **87**, 192501 (2001).
 - [5] Y. Liu and Y.-L. Ye, *Nucl. Sci. Tech.* **29**, 184 (2018).
 - [6] F. Hoyle, *The Astrophysical Journal Supplement Series* **1**, 121 (1954).
 - [7] Z. Ren and B. Zhou, *Frontiers of Physics* **13**, 132110 (2018).
 - [8] W. Vonoertzen, M. Freer, and Y. Kanadaenyo, *Physics Reports* **432**, 43 (2006).
 - [9] W. B. He, Y. G. Ma, X. G. Cao, X. Z. Cai, and G. Q. Zhang, *Physical Review Letters* **113**, 032506 (2014).
 - [10] E. R. Arriola and W. Broniowski, *Journal of Physics: Conference Series* **630**, 012060 (2015).
 - [11] M. Rybczyński, M. Piotrowska, and W. Broniowski, *Physical Review C* **97**, 034912 (2018).
 - [12] C. Z. Shi and Y. G. Ma, *Nucl. Sci. Tech.* **32**, 66 (2021).
 - [13] B. S. Huang, Y. G. Ma, and W. B. He, *Physical Review C* **95**, 034606 (2017).
 - [14] B.-S. Huang and Y.-G. Ma, *Physical Review C* **101**, 034615 (2020).
 - [15] W. Broniowski and E. Ruiz Arriola, *Physical Review Letters* **112**, 112501 (2014).
 - [16] D. Teaney and E. V. Shuryak, *Physical Review Letters* **83**, 4951 (1999).
 - [17] C. Gale, S. Jeon, and B. Schenke, *International Journal of Modern Physics A* **28**, 1340011 (2013).
 - [18] C. Shen and L. Yan, *Nucl. Sci. Tech.* **31**, 122 (2020).
 - [19] S. Wu, C. Shen, and H. Song, *Chin. Phys. Lett.* **38**, 081201 (2021).
 - [20] P. Bożek, W. Broniowski, E. R. Arriola, and M. Rybczyński, *Physical Review C* **90**, 064902 (2014).
 - [21] S. Zhang, Y. G. Ma, J. H. Chen, W. B. He, and C. Zhong, *Physical Review C* **95**, 064904 (2017).
 - [22] N. Summerfield, B.-N. Lu, C. Plumberg, D. Lee, J. Noronha-Hostler, and A. Timmins, **104**, L041901.
 - [23] X.-N. Wang, *Physical Review C* **63**, 054902 (2001).
 - [24] H. Agakishiev *et al.* (STAR Collaboration), *Chinese Physics C* **45**, 044002 (2021).
 - [25] H. Agakishiev *et al.* (STAR Collaboration), *Physical Review C* **89**, 041901 (2014).
 - [26] A. Adare *et al.* (PHENIX Collaboration), *Physical Review C* **99**, 054903 (2019).
 - [27] C. Adler *et al.* (STAR Collaboration), *Physical Review Letters* **90**, 082302 (2003).
 - [28] J. Adams *et al.* (STAR Collaboration), *Physical Review Letters* **93**, 252301 (2004).
 - [29] J. Ulery, *Nuclear Physics A* **774**, 581 (2006).
 - [30] N. N. Ajitanand, J. M. Alexander, P. Chung, *et al.*, *Physical Review C* **72**, 011902 (2005).
 - [31] G. L. Ma, S. Zhang, Y. G. Ma, *et al.*, *Physics Letters B* **641**, 362 (2006).
 - [32] S. S. Adler *et al.* (PHENIX Collaboration), *Physical Review Letters* **97**, 052301 (2006).

- [33] M. M. Aggarwal *et al.* (STAR Collaboration), *Physical Review C* **82**, 024912 (2010).
- [34] L. Adamczyk *et al.* (STAR Collaboration), *Physics Letters B* **751**, 233 (2015).
- [35] M. Aaboud *et al.* (ATLAS Collaboration), *The European Physical Journal C* **78**, 997 (2018).
- [36] S. Chatrchyan *et al.* (CMS Collaboration), *The European Physical Journal C* **72**, 2012 (2012).
- [37] G. Aad *et al.* (ATLAS Collaboration), *Physical Review Letters* **110**, 182302 (2013).
- [38] G. Aad *et al.* (ATLAS Collaboration), *Physical Review Letters* **116**, 172301 (2016).
- [39] ALICE Collaboration, *Nature Physics* **13**, 535 (2017).
- [40] W. Li, S. Zhang, Y. G. Ma, X. Z. Cai, J. H. Chen, H. Z. Huang, G. L. Ma, and C. Zhong, *Phys. Rev. C* **80**, 064913 (2009).
- [41] M. Nie, L. Yi, X. Luo, G. Ma, and J. Jia, *Physical Review C* **100**, 064905 (2019).
- [42] S. Zhang, Y. Ma, G. Ma, J. Chen, Q. Shou, W. He, and C. Zhong, *Physics Letters B* **804**, 135366 (2020).
- [43] Z.-W. Lin, C. M. Ko, B.-A. Li, B. Zhang, and S. Pal, *Phys. Rev. C* **72**, 064901 (2005).
- [44] STAR Collaboration, “The star beam use request for run-20 and run-21,” (2019), https://drupal.star.bnl.gov/STAR/files/BUR2019_final_0_0.pdf.
- [45] Z. Citron, A. Dainese, J. F. Grosse-Oetringhaus, J. M. Jowett, Y.-J. Lee, and U. A. Wiedemann, *CERN Yellow Rep.: Monogr.* **7**, 1159 (2019).
- [46] Z.-W. Lin and L. Zheng, *Nucl. Sci. Tech.* **32**, 113 (2021).
- [47] X.-N. Wang and M. Gyulassy, *Phys. Rev. D* **44**, 3501 (1991).
- [48] M. Gyulassy and X.-N. Wang, *Computer Physics Communications* **83**, 307 (1994).
- [49] B. Zhang, *Computer Physics Communications* **109**, 193 (1998).
- [50] B.-A. Li and C. M. Ko, *Phys. Rev. C* **52**, 2037 (1995).
- [51] G.-L. Ma and Z.-W. Lin, *Phys. Rev. C* **93**, 054911 (2016).
- [52] H. Wang and J. H. Chen, *Nucl. Sci. Tech.* **32**, 2 (2021).
- [53] H. Wang, J. H. Chen, Y. G. Ma, *et al.*, *Nucl. Sci. Tech.* **30**, 185 (2019).
- [54] A. H. Tang, *Chin. Phys. C* **44**, 054101 (2020).
- [55] T. Maruyama, K. Niita, and A. Iwamoto, *Physical Review C* **53**, 297 (1996).
- [56] I. Angeli and K. Marinova, *Atomic Data and Nuclear Data Tables* **99**, 69 (2013).
- [57] Y.-A. Li, S. Zhang, and Y.-G. Ma, *Physical Review C* **102**, 054907 (2020).
- [58] Y.-A. Li, D.-F. Wang, S. Zhang, and Y.-G. Ma, *Phys. Rev. C* **104**, in press (2021).
- [59] M. Connors, C. Nattrass, R. Reed, and S. Salur, *Reviews of Modern Physics* **90**, 025005 (2018).
- [60] M. Gyulassy and X.-N. Wang, *Computer Physics Communications* **83**, 307 (1994).
- [61] N. Armesto, C. A. Salgado, and U. A. Wiedemann, *Physical Review Letters* **93**, 242301 (2004).
- [62] S. Zhang, Y. H. Zhu, G. L. Ma, Y. G. Ma, X. Z. Cai, J. H. Chen, and C. Zhong, *Nuclear Physics A* **860**, 76 (2011).
- [63] G.-L. Ma and X.-N. Wang, *Physical Review Letters* **106**, 162301 (2011).
- [64] G. L. Ma, S. Zhang, Y. G. Ma, X. Z. Cai, J. H. Chen, and C. Zhong, *The European Physical Journal C* **57**, 589 (2008).
- [65] J. Adams *et al.* (STAR Collaboration), *Physical Review Letters* **95**, 152301 (2005).
- [66] A. M. Poskanzer and S. A. Voloshin, *Physical Review C* **58**, 1671 (1998).
- [67] S. A. Voloshin, A. M. Poskanzer, A. Tang, and G. Wang, *Physics Letters B* **659**, 537 (2008).
- [68] L. Ma, Y. G. Ma, and S. Zhang, *Physical Review C* **102**, 014910 (2020).
- [69] K. Xiao, F. Liu, and F. Wang, *Physical Review C* **87**, 011901 (2013).
- [70] M. Nie, *Nuclear Physics A* **982**, 403 (2019).